A New Ocean SAR Imaging Process Simulator

Morgan Lamy, Jean-Marc Le Caillec and René Garello
GET - ENST Bretagne
CNRS FRE 2658 TAMCIC Equipe TIME
Technopôle Brest Iroise, CS 83818
29238 BREST Cedex - FRANCE
Email: morgan.lamy@enst-bretagne.fr

Ali Khenchaf
ENSIETA
Dept E^3I^2
2, rue François Verny
29806 BREST Cedex 09 - FRANCE

***Abstract*— In this paper we develop the concept of a new ocean SAR imaging simulator. We intend to come up with a simulator more complete than those which have been developed until now. Indeed, in addition to the large number of oceanic and atmospheric phenomena considered, the simulator should lead to cope with various radar configurations (spaceborne, airborne, grazing-angle).**

The simulator is based on several interconnected units allowing to model the sea surface features and their interactions with the radar electromagnetic waves. We develop the hydrodynamic modulation of the short waves by the long waves which are at the core of the process. The peculiarities of different type of radars and radar carriers are also included.

I. Introduction

Synthetic Aperture Radar (SAR) is a very useful instrument for studying, observing and monitoring the ocean. Since its first experiment on board aircraft in the 60's, the knowledge on the mechanisms leading to the formation of a sea surface image has been constantly improved. Many models have been developed which allow to understand more accurately the transfers between oceanic phenomena and sea surface, between the surface and the radar wave as well as the aperture synthesis processing itself.

Although SAR imaging models of waves, internal waves, oil slicks etc... give generally good results, they fail in some cases.

In order to understand more precisely the mechanisms of SAR ocean imaging we have started developing a simulator which includes a large number of oceanic features using existing models. This allows us to test and hopefully to improve these models. The simulator must be able to simulate images acquired by SAR, by Real Aperture Radar (RAR) or by grazing-angle radar such as those carried aboard search and rescue unit planes.

This paper presents the simulator structure (section II) and preliminary results concerning the simulation of swell imaging process using a linear hydrodynamic modulation transfer function associated with the spectrum developed in [13] (section III).

II. The simulator

SAR imaging simulators are useful for many reasons. First of all, they allow to emphasize the role and the sensitivity of SAR parameters (band, polarization, incidence angle, spaceborne/airborne, ...). A SAR system does not image phenomena in the same way when it operates in C-band or in P-band, in vertical polarization (VV) or horizontal polarization (HH). Secondly, simulators are used to test and to validate inversion algorithms. They make it possible to improve the overall knowledge on oceanic and atmospheric phenomena. Finally, they are useful in mission preparation.

Many ocean SAR imaging models exist. Some of them, like those compared in [1], deal only with the imaging of the waves, with underwater topography [15] or with internal waves. Unfortunately, few simulators gather together these different models in order to take into account the large number of phenomena present in and at the surface of the ocean.

As said in the introduction, we plan to design a complete simulator. It has to integrate many oceanic phenomena such as ocean waves, wave breaking, internal waves, ships (structure and wake), topographic effects, eddies and oil slicks. Atmospheric phenomena have to be taken into account as well. In addition to the large number of phenomena which should be incorporated, the simulator has to be able to test several instrument configurations like spaceborne and airborne SARs, but also grazing-angle radars such as those operated in search and rescue unit planes. It has also to be sufficiently adaptable in order to give the possibility of incorporating new models in it and to test them.

For all these reasons, a simulator based on three main units was developed.

- Surface feature modeling unit: includes modelling of the ocean surface, of oceanic and atmospheric phenomena, and of interactions between these phenomena,
- Electromagnetic modeling unit: the modeling of the interaction between the radar wave and the sea surface,
- SAR processing modeling: includes the motion of the scatterers ("velocity bunching", "azimut smearing", ...)

The scheme of the simulator is introduced by figure 1 and the following paragraphs give a more detailed description of the three sets.

A. The surface feature modeling unit

This set deals with the modeling of the marine and the atmospheric environment, and reproduces the sea surface modulations which, in association with the electromagnetic

0-933957-31-9

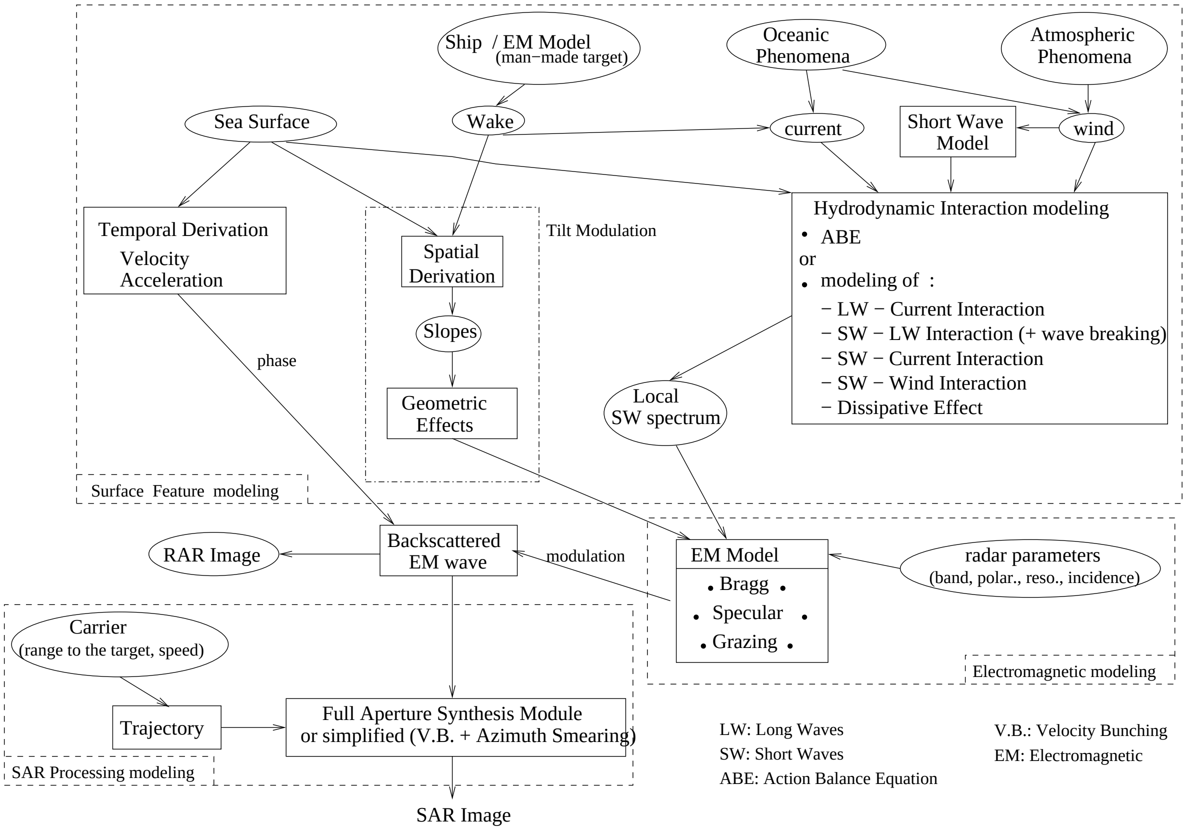

Fig. 1. Flowchart of the ocean surface SAR imaging simulator

modeling, lead to the radar wave modulation. It also produces the Doppler characteristics of the backscattered wave.

The marine environment is composed of the short waves which are responsible of the radar wave backscattering, the ocean surface (i.e. the long waves) and the oceanic phenomena. The latter gathers together a number of phenomena: internal waves, underwater topography, oceanic fronts, eddies, ships wakes... They take part in various ways in the modification of the sea surface: they generate and modulate surface currents, they modulate the wind stress, they are forcing an elevation of the surface.

The atmospheric environment mainly acts on the sea surface by mean of the wind at the boundary-layer. The wind is modified by atmospheric phenomena such as atmospheric internal waves or convective cells for instance. It is an important parameter because it enters in the modeling of the short waves [13] which play an important role in the backscattering of the radar wave.

Many interactions are present at the sea surface. We gather them together into the module called *Hydrodynamic Interaction Modeling*. We put into this module the interactions between long waves and current, short waves and current, short waves and long waves, wind and waves, and the dissipative effects. These different interactions are not yet completely understood, and thus are the subject of ongoing researches. This case is an example of the usefulness of our simulator allowing to test and to validate the hydrodynamic interaction models which are regularly developed.

Thanks to this module, we obtain the local variations of the short wave spectrum caused by the acceleration and the velocity of the long waves, and by current changes. Coupled with an adequate electromagnetic model, these variations provide the hydrodynamic modulation of the backscattered wave.

The other modulation of the backscattered wave which is included in the surface feature modeling is the so-called tilt modulation. In this mechanism, the modulation of the return wave is linked to the modulation of the short waves by the long waves. It depends particularly on the local incidence angle of the radar wave which is modified by the surface slopes. In order to simulate this effect, we have first of all to calculate the spatial derivatives of the surface elevation to obtain the surface slopes [3]. These slopes lead to geometric effects which, together with the electromagnetic model, yield the tilt modulation of the backscattered wave.

From the calculation of tilt and hydrodynamic modulations, we get the variations of intensity of the backscattered wave, and thus the image of the sea surface such as it would have been acquired by a RAR. The variation of the returned signal phase is necessary in order to carry out the simulation of the aperture synthesis, . It is obtained from velocity and acceleration of the sea surface, which are temporal derivatives of the surface elevation [3].

B. The electromagnetic modeling unit

The electromagnetic modeling reproduces the interaction between incident radar wave and sea surface. In our case of monostatic radar, this module models the backscattering of electromagnetic wave.

Two main mechanisms are responsible for the radar wave backscattering: the specular reflection and the Bragg resonance. The predominance of one on the other depends on the incidence angle of the radar wave.

For low incidence angles, i.e. between $0°$ and $20-30°$, the specular reflection has to be considered [11]. In this case, the Kirchhoff's method which assumes the tangent plane approximation is generally used. The sea surface is thus decomposed into plane facets, and the surface reflection depends on the number of facets normal to the direction of incident radiation.

For moderate incidence angles, i.e. between $20-30°$ and $70°$, it is generally accepted that the Bragg resonance is the dominant mechanism [11]. The electromagnetic waves enter in resonance with ocean waves called Bragg waves of half the electromagnetic wavelength. To first order, the backscattered power is proportional to the spectral density of these short waves. Nevertheless, all the phenomena are not explained by this simplified theory. Some authors have developed more sophisticated theories, based on Bragg theory, integrating furthermore the impact of the whole wave spectrum into the backscattered power [9], [10].

For large incidence angles, other phenomena like shadowing and diffraction are added and can play a significative role [11].

Although the majority of spaceborne radars have got a moderate incidence angle (ERS-1 $23°$, RADARSAT between $20°$ and $49°$, JERS $35°$ ...), airborne radars can be used to operate at low, moderate or large angle, and radars of patrol planes have generally a grazing incidence. The simulator has to consider all these applications and must be able to model the radar/surface interaction for all incidence angles.

In addition to the incidence angle which determines the type of electromagnetic model, other parameters are needed. They mainly are parameters defining the radar: wavelength and polarization of the transmitted wave, and radar resolution.

C. The radar processing modeling unit

The step of the synthesis of the aperture can be simulated by several methods. The more concise and complete one consists of applying the so-called focusing method from the sea surface return. This implies to simulate the range-doppler images of the sea surface. Obviously,this method is the more appropriate for understanding the whole SAR transform. However, since one goal of the simulator is to be modular, this step can be simplified by taking directly into account the phenomena induced by the synthetic aperture such as "Velocity Bunching" and "Azimuth Smearing". Results presented in section III-B have been obtained by using this latter method which is the fastest one.

III. Hydrodynamic modulation of short waves by long waves

In the framework of the development of the simulator, we first of all work on ocean wave imaging and in particular on swell imaging. To do so, we have to model the interaction of short waves, responsible of the backscattering, with the long waves. We re-use here the theory presented in [14] and [6] with some modifications to introduce Elfouhaily spectrum [13]. Results are presented for the simulation of images acquired by three different radars (ERS-1/2, RADARSAT, airborne) and for two different sea states.

A. Theory

Local variations of the short wave spectrum are due to the acceleration and the velocity of the long waves. This phenomenon was modelled in [14] using the action balance equation. The action spectrum $N(\underline{x},\widehat{\underline{k}},t)$ is linked to the short wave spectrum $S(\underline{x},\widehat{\underline{k}},t)$, for a given wavenumber $\widehat{\underline{k}}$, by the following relation:

$$N(\underline{x},\widehat{\underline{k}},t) = S(\underline{x},\widehat{\underline{k}},t)/\omega' \tag{1}$$

where ω' is the frequency of the short wave in a reference system moving with the long waves. We distinguish the wavenumber $\widehat{\underline{k}}$ and the frequency $\widehat{\omega}$ of the short waves and the corresponding quantities $\underline{k}$ and ω of the long waves.

The action balance equation relates the variations of action (therefore the variations of short wave spectrum) to a source function which models the different energy transfers: input from wind onto the sea, energy transfers within the wave field, dissipative processes. This function is not yet known with accuracy [14], therefore we are making several assumptions. First of all, the perturbations due to the long waves are small around an equilibrium state. It allows a linear development around this equilibrium state. Then, we consider the derivative of the source function, at the equilibrium state, as a diagonal operator. Thanks to these two assumptions, the hydrodynamic modulation transfer function of the short waves by the long waves [14] is given by:

$$T^{Hyd}(\underline{k}) = \frac{\omega - j\mu}{\omega^2+\mu^2}\cdot\frac{\underline{k}.\widehat{\underline{k}}}{|\underline{k}|}.\omega.\left[\frac{1}{S(\underline{k})}.\underline{k}.\frac{\partial S(\widehat{\underline{k}})}{\partial\widehat{\underline{k}}} - \gamma(\widehat{\underline{k}})\cdot\frac{\widehat{\underline{k}}.\underline{k}}{|\widehat{\underline{k}}|^2}\right] \tag{2}$$

with $\mu^{-1}(\widehat{\underline{k}},\underline{x})$ the relaxation rate of the system introduced by the source term and $\gamma(\widehat{\underline{k}}) = \frac{1}{2}.\frac{1+3.\frac{\tau}{\rho.g}.|\widehat{\underline{k}}|^2}{1+\frac{\tau}{\rho.g}.|\widehat{\underline{k}}|^2}$.

Using Phillips spectrum [7] and assuming that the electromagnetic wave is carried by the y axis ($\underline{\widehat{k}} = \widehat{k}.\underline{y}$), the following expression [6], [14] is found for the hydrodynamic modulation transfer function:

$$T^{Hyd}_{A-H}(k) = -k\,.\,\omega\,.\,(4+\gamma(\widehat{k}))\,.\,\left(\frac{k_y^2}{k^2}\right)\,.\,\frac{\omega - j\mu}{\omega^2+\mu^2} \qquad (3)$$

In [6], the authors report results of Feindt's thesis [2] (available only in German). This author finds a more accurate relation with laboratory measurements by adding in (3) a feedback term for the wind which must be determined heuristically. So (3) becomes:

$$T^{Hyd}_{Feindt}(k) = -k\,.\,\omega\,.\,(4+\gamma(\widehat{k}))\,.\,\left(\frac{k_y^2}{k^2} + Y_r + j\,.\,Y_i\right)\,.\,\frac{\omega - j\mu}{\omega^2+\mu^2} \qquad (4)$$

Phillips spectrum [7] is used intensively in the literature because of its simple formulation. Unfortunately it does not satisfy measurements. Other models of spectra have been developed and agree more precisely with observations. One of them is the Elfouhaily spectrum [13]. This spectrum has a relatively simple analytic form. It relies on Phillips [8] and Kitaigorodskii [12] works for the high frequency regime and on the JOint Norh Sea WAve Project (JONSWAP, [5]) for the long wave regime. Here we use the expression of the Elfouhaily spectrum for the short waves:

$$S_{Elfouhaily}(\widehat{k}) = \frac{1}{2} c_m \alpha_m \widehat{k}^{-3} \frac{1}{c(\widehat{k})} \exp[-\frac{1}{4}(\frac{\widehat{k}}{k_m} - 1)^2] \qquad (5)$$

where k_m is the gravity-capillarity peak of the curvature spectrum $\widehat{k}^3 S$ ($k_m = 370$ rad/m), $c(\widehat{k})$ the phase speed, c_m the phase speed at the peak and α_m a parameter which depends of the friction velocity of the wind.

Introducing (5) in (2) and considering the electromagnetic wave directed in the y axis, the hydrodynamic modulation transfer function is given by:

$$T^{Hyd}_{Elf}(k) = -\omega\,.\,\left[3 - \tfrac{1}{2}\Gamma(\widehat{k}) - \tfrac{\widehat{k}}{2k_m}\left(1 - \tfrac{\widehat{k}}{k_m}\right) + \gamma k\right] \cdot \tfrac{k_y^2}{k^2} \cdot \tfrac{\omega - j\mu}{\omega^2+\mu^2} \qquad (6)$$

with $\Gamma(\widehat{k}) = \frac{1-\frac{\tau}{\rho g}\widehat{k}^2}{1+\frac{\tau}{\rho g}\widehat{k}^2}$.

B. Applications

In order to simulate SAR images of swell, we have implemented the process detailed in this paragraph.

First the sea surface is generated from the JONSWAP spectrum [5]. For that the square root of the spectrum is multiplied by a joint complex Gaussian random variable with unit variance. Thus a random variable with a variance equal to the spectrum is obtained. The tilt modulation modeling described in [4] and the hydrodynamic modulation models previously presented in eq. (4) and (6) are then applied to this sea surface. In order to complete these equations, we take $\mu(k,\widehat{k}) = (0.04\,U_{10}\,\frac{dk}{d\omega})\widehat{\omega}$, the feedback term $Y_r + jY_i = \mu\frac{dk}{d\omega}e^{j\varphi}$ with $\varphi = \frac{\pi}{4}$ and the wind $U_{10} = 10m.s^{-1}$.

We obtain a simulated image of the sea surface as it would be acquired by a RAR. Then, in order to simulate the radar processing, we apply to the RAR image the velocity bunching transfer function and a model of speckle noise.

C. Results

The simulation method has been applied to two specific sea states the parameters of which are given in table I. They correspond to two cases of swell which propagates respectively in the range direction and in the azimuth direction.

	Sea state 1	Sea state 2
Predominant wavelength	$200m$	$300m$
Significant wave height	$3m$	$7m$
Wave direction/range axis	$0°$	$90°$

TABLE I
SEA STATE PARAMETERS

Three radar configurations are tested (Table II): ERS, RADARSAT and a case of airborne SAR.

	ERS	RADARSAT	Airborne
Band	C	C	P
θ_i	23°	35°	45°
Polarization	VV	HH	VV
R/V	115	120	80

TABLE II
RADAR CONFIGURATIONS FOR THE SIMULATIONS

Results of the simulation are showed in figure 2. Because of the similarities between the simulated images obtained using the Elfouhaily spectrum [13] in the hydrodynamic modulation (eq. (6)) and using equation (4), we present only one set of images.

Unexpectedly, few differences are found between the simulations (for a given sea state), in particular between airborne and spaceborne simulations. This can be explain in part by the fact that we have neglected a specific SAR mechanism, the scanning distortion. This latter is due to the sea motion during the image construction. Its effect is proportional to the ratio between the phase velocity of the predominant wavelength and the radar speed, and so can be neglected for spaceborne simulations but must be included in airborne simulations.

IV. DISCUSSION

Some phenomena are not present in figure 1. Among them we can quote oil spills or floating ice. These phenomena will soon be incorporated in the simulator. Nevertheless, the simulation of different features is not the more drastic problem encountered in the simulator construction. In fact, there are lots of realistic/unrealistic and complicated/simple models for each of the marine feature described above. The real challenge of the simulator will consist of taking into account several feature occurring on the same image, such as long wave/internal wave, long wave/wake/wind… For instance, the simulation of a ship must include the ship backscattering, the wave backscattering and double bounce (ship-sea and sea-ship) backscattering. A way to proceed consists of deriving new models conveying the marine feature backscattering and the interactions between these features. However, due to the large number of features assumed to be included in the simulator, this could be a tedious task.

V. Conclusion

The project of a modular ocean SAR imaging process simulator hopefully more complete has been presented. We pretend that it is complete because it takes into account a larger number of phenomena (oceanic, atmospheric, electromagnetic). Its modularity allows us to interchange the different models which are used, in order to test them, validate them and compare them with other.

There is no doubt on the usefulness of such a simulator. It will let us test and validate inversion algorithms, highlight the role and the sensibility of radar parameters, help to prepare missions, …

A detailed flowchart of the simulator has been presented. However, some modifications have to be introduced, we especially will come up with the incorporation of oil spills modeling.

The development of the simulator has just begun, nevertheless simulations of sea surface SAR images have been carried out. A particular modeling of hydrodynamic modulation have been used. Considering the results, it is clear that improvements have to be done in order to produce more realistic images. We have to obtain the same differences that are noticed in the comparisons between images acquired by different radar configurations.

When these modifications are carried out, more realistic sea surface SAR images will be obtained. We will then start to perform internal wave modeling and we will study the effects of these waves on SAR imaging. It will be the first stage of the modeling of oceanic phenomena.

References

[1] Kasilingam D.P. and O.H. Shemdin. Models for synthetic aperture radar imaging of the ocean: a comparison. *J. Geophys. Res.*, 95:16263–16276, 1990.

[2] Feindt F. *Ruckstreuexperimente am Wind-Wellen-Kanal bei sauberer und filmbedeckter Wasseroberflache im X-Band (9.8 Ghz)*. Ph.D. Thesis, Hamburg Univ., Germany, 1985.

[3] Lamb H. *Hydrodynamics*. Dover, New York, 6th edition, 1932.

[4] Wright J.W. A new model of sea clutter. *IEEE Trans. Antennas Propagat.*, AP-16:217–223, 1968.

[5] Hasselmann K., T.P. Barnett, E. Bouws, H. Carlson, D.E. CartWright, K. Enke, J.A. Ewing, H. Gienapp, D.E. Hasselmann, P. Kruseman, A. Meerburg, P. Mueller, D.J. Olbers, K. Richter, S. Sell, and H. Walden. Measurements of wind-wave growth and swell decay during the Joint North Sea Wave Project (JONSWAP). *Deutsche Hydrographische Zeitschrift*, Reihe A(12):1–95, 1973.

[6] Hasselmann K. and S. Hasselmann. On the nonlinear mapping of an ocean wave spectrum into a synthetic aperture radar image spectrum and its inversion. *J. Geophys. Res.*, 96(C6):10713–10729, 1991.

[7] Phillips O. M. *The dynamics of the Upper Ocean*. Cambridge, Cambridge University Press, 2nd edition, 1977.

[8] Phillips O.M. Spectral and statistical properties of the equilibrium range in wind-generated gravity waves. *J. Fluid Mech.*, 156:505–531, 1985.

[9] Lyzenga D. R. and J. R. Bennett. Full-spectrum modeling of synthetic aperture radar internal waves signatures. *J. Geophys. Res.*, 93(C10):12345–12354, 1988.

[10] Romeiser R., W. Alpers, and V. Wismann. An improved composite model for the radar backscattering cross section of the ocean surface. 1. theory of the model and optimization/validation by scatterometer data. *J. Geophys. Res.*, 102(25):237–250, 1997.

[11] Valenzuela G. R. Theories for the interaction of electromagnetic and oceanic waves - a review. *Boundary-Layer Meteorology*, 13:61–85, 1978.

[12] Kitaigorodskii S.A. *The Physics of Sea-Air Interactions*. Keter-Press, Jerusalem, 1973.

[13] Elfouhaily T., B. Chapron, K. Katsaros, and D. Vandermark. A unified directional spectrum for long and short wind-driven waves. *IEEE Trans. Geosci. Remote Sensing*, 102(C3):15781–15796, July 1997.

[14] Alpers W. and K. Hasselmann. The two-frequency microwave technique for measuring ocean-wave spectra from an airplane or satellite. *Boundary-Layer Meteorology*, 13:215–230, 1978.

[15] Alpers W.R. and I. Hennings. A theory of the imaging mechanism of underwater bottom topography by real and synthetic aperture radar. *J. Geophys. Res.*, 89(6):10529–10546, November 1984.

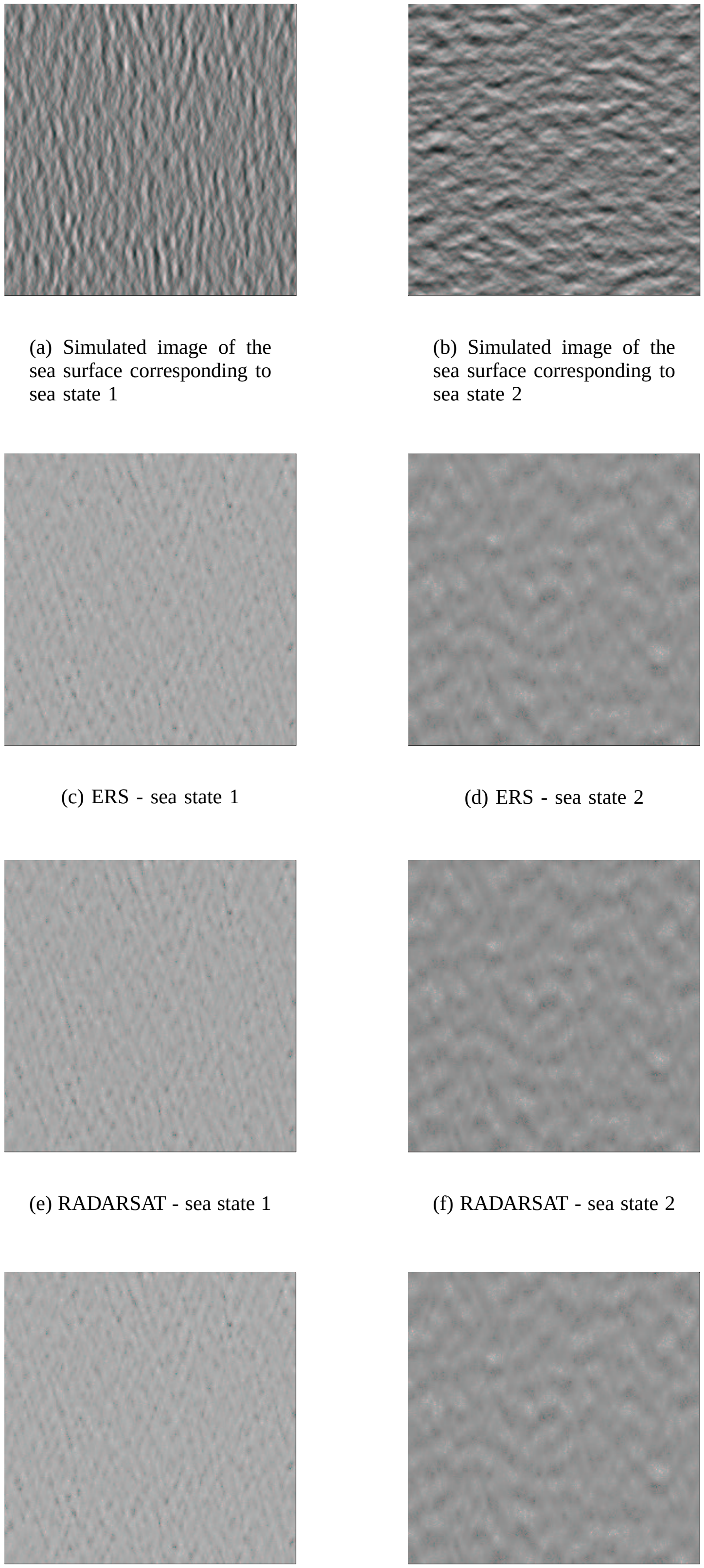

(a) Simulated image of the sea surface corresponding to sea state 1

(b) Simulated image of the sea surface corresponding to sea state 2

(c) ERS - sea state 1

(d) ERS - sea state 2

(e) RADARSAT - sea state 1

(f) RADARSAT - sea state 2

(g) Airborne - sea state 1

(h) Airborne - sea state 2

Fig. 2.
(a) and (b): Ocean surface simulation
(c)-(h) SAR simulated images for several radar configurations